J|A|C|S
ARTICLES
Published on Web 08/25/2007

Thermally Activated Electron Transport in Single Redox Molecules

Xiulan Li,[†] Joshua Hihath,[†] Fang Chen,[†] Takuya Masuda,[†] Ling Zang,[‡] and Nongjian Tao*,[†]

Contribution from the Department of Electrical Engineering and Center for Solid State Electronic Research, Arizona State University, Tempe, Arizona 85287, and Department of Chemistry and Biochemistry, Southern Illinois University, Carbondale, Illinois 62901

Received May 4, 2007; E-mail: nongjian.tao@asu.edu

Abstract: We have studied electron transport through single redox molecules, perylene tetracarboxylic diimides, covalently bound to two gold electrodes via different linker groups, as a function of electrochemical gate voltage and temperature in different solvents. The conductance of these molecules is sensitive to the linker groups because of different electronic coupling strengths between the molecules and electrodes. The current through each of the molecules can be controlled reversibly over 2−3 orders of magnitude with the gate and reaches a peak near the redox potential of the molecules. The similarity in the gate effect of these molecules indicates that they share the same transport mechanism. The temperature dependence measurement indicates that the electron transport is a thermally activated process. Both the gate effect and temperature dependence can be qualitatively described by a two-step sequential electron-transfer process.

Introduction

A basic task in molecular electronics is to understand electron transport through a single molecule bridged across two electrodes.[1,2] To date, most studies have focused on systems where the Fermi levels of the metal electrodes lie in the LUMO−HOMO gap and far away from the LUMO and HOMO levels of the molecule. In this case, electron transport is described by a coherent tunneling or superexchange process, and good quantitative agreement between theories and experiments has been found for many molecular systems.[3] However, large thermal fluctuations of nucleic coordinates, including conformational changes in the molecule and polarization of the solvent molecules surrounding the molecule, can play a critical role in the electron transport of the molecule in more general cases.[4−6] It has been argued that when the tunneling traversal time is comparable to the time scale of the nucleic motions, tunneling electrons interact strongly with the nucleic coordinates and lead to a thermally activated hopping mechanism in electron transport through molecules.[4] Thermal activation has been well studied in various electron-transfer reactions taking place at electrode−solution interfaces, but it is much less explored in electron transport through a single molecule bridged between two electrodes. The goal of the present work is to study thermally activated electron transport in single redox molecules by controlling various key parameters.

Redox molecules are attractive for this purpose because their LUMO (or HOMO) levels are often close to the Fermi levels of metal electrodes. Furthermore, one can shift and align the molecular energy levels to the Fermi levels by adjusting the electrochemical gate potential. Since the tunneling traversal time is inversely proportional to the energy difference between the LUMO (or HOMO) and Fermi levels, a strong coupling between the electronic and nucleic motions is expected in electron transport of redox molecules.[7] Redox molecules are also attractive for molecular electronics because they can be reversibly oxidized and reduced by controlling the electrochemical gate voltage, leading to field effect transistor-like behavior.[8−11] Several groups have reported electrochemical gate-modulated electron transport in single redox molecules using different techniques.[12−17]

[†] Arizona State University.
[‡] Southern Illinois University.

(1) Nitzan, A.; Ratner, M. A. *Science* **2003**, *300*, 1384−1389.
(2) Tao, N. J. *Nat. Nanotechnol.* **2006**, *1*, 173−181.
(3) Lindsay, S. M.; Ratner, A. M. *Adv. Mater.* **2007**, *19*, 23−31.
(4) Segal, D.; Nitzan, A.; Ratner, M. A.; Davis, W. B. *J. Phys. Chem. B* **2000**, *104*, 2790−2793.
(5) Haiss, W.; van Zalinge, H.; Bethell, D.; Ulstrup, J.; Schiffrin, D. J.; Nichols, R. J. *Faraday Discuss.* **2006**, *131*, 253−364.
(6) Selzer, Y.; Cabassi, M. A.; Mayer, T. S.; Allara, D. L. *J. Am. Chem. Soc.* **2004**, *126*, 4052−4053.
(7) Nitzan, A.; Jortner, J.; Wilkie, J.; Burin, A. L.; Ratner, M. A. *J. Phys. Chem. B* **2000**, *104*, 5661−5665.
(8) Schmickler, W.; Widrig, C. *J. Electroanal. Chem.* **1992**, *336*, 213−221.
(9) Di Ventra, M.; Pantelides, S. T.; Lang, N. D. *Appl. Phys. Lett.* **2000**, *76*, 3448−3450.
(10) Kuznetsov, A. M.; Ulstrup, J. *J. Phys. Chem. A* **2000**, *104*, 11531−11540.
(11) Su, W.; Jiang, J.; Lu, W.; Luo, Y. *Nano Lett.* **2006**, *6*, 2091−2094.
(12) Haiss, W.; van Zalinge, H.; Higgins, S. J.; Bethell, D.; Hoebenreich, H.; Schiffrin, D. J.; Nichols, R. J. *J. Am. Chem. Soc.* **2003**, *125*, 15294−15295.
(13) Xu, B.; Xiao, X.; Yang, X.; Zang, L.; Tao, N. *J. Am. Chem. Soc.* **2005**, *127*, 2386−2387.
(14) Chen, F.; He, J.; Nuckolls, C.; Roberts, T.; Klare, J. E.; Lindsay, S. *Nano Lett.* **2005**, *5*, 503−506.
(15) Albrecht, T.; Guckian, A.; Ulstrup, J.; Vos, J. G. *Nano Lett.* **2005**, *5*, 1451−1455.
(16) Tao, N. J. *Phys. Rev. Lett.* **1996**, *76*, 4066−4069.
(17) Gittins, D. I.; Bethell, D.; Schiffrin, D. J.; Nichols, R. J. *Nature* **2000**, *408*, 67−69.

Scheme 1

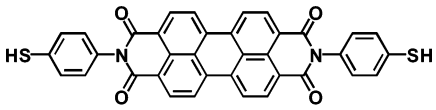

T-PTCDI

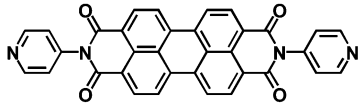

P-PTCDI

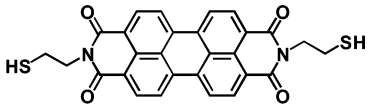

C-PTCDI

In addition to temperature, gate voltage, and environment, another parameter that controls electron transport in molecules is the contact between the redox center and the electrodes. The important role of molecule−electrode contact in the conductance of non-redox molecules has been recognized and discussed in the literature.[18−21] In the case of redox molecules, the contact affects the electronic coupling strength between the redox center and the electrodes, and thus the tunneling traversal time. Here we report on a study of electron transport in single redox molecules by changing temperature, electrochemical gate voltage, solvent, and redox center-electrode coupling strength via different anchoring groups.

Experimental Section

The redox molecules studied here are perylene tetracarboxylic diimide (PTCDI) derivatives (Scheme 1). These molecules are terminated with ethylthiols, phenylthiols, or pyridines that provide anchoring groups for them to bind to Au electrodes with different binding strengths and form electrode−molecule−electrode junctions. The three PTCDI molecules were synthesized following the same method as described elsewhere.[13] Before each measurement, an appropriate amount of PTCDI solid was dispersed in dimethyl sulfoxide (DMSO) upon sonication to reach a saturated suspension, in which the molecule can be dissolved at concentrations of a few micromolar. The Au electrodes were prepared by thermally evaporating ~130 nm gold (99.999%, Alfa Aesar) on freshly cleaved mica slides (Ted Pella) in a UHV chamber ($\sim 5 \times 10^{-8}$ Torr). Before each measurement, a Au electrode was annealed in a hydrogen flame briefly to remove contamination and to form an atomically flat surface and then immediately immersed in the DMSO solution overnight to allow PTCDI molecules to adsorb onto the surface. The Au electrode covered with PTCDI molecules was thoroughly rinsed and brought into contact with either nonpolar toluene or 0.1 M $NaClO_4$ aqueous electrolyte for electron transport measurements. The electrolyte provided a polar environment and also allowed electrochemical gate control.

We used a scanning tunneling microscope (STM) break junction approach to measure electron transport in single molecules.[22] The setup was a modified Pico-STM (Molecular Imaging Corp.) using a home-made control system. Two linear current preamplifiers with gains of 10 and 1 nA/V as well as a logarithmic amplifier were used to cover the large current range required for the molecules. The molecular junctions of the PTCDI derivatives were formed by bridging the molecules between a Au STM tip and a Au substrate. The tip was a freshly cut 0.25-mm gold wire (99.998%, Alfa Aesar) that was coated with Apiezon wax to minimize ionic leakage current in the electrolyte. The leakage was found to be ~1 pA or less in 0.1 M $NaClO_4$, much smaller than the electron transport current through the PTCDI molecules measured here. The cyclic voltammograms of the PTCDI derivatives adsorbed on Au electrodes were obtained with a potentiostat (Cypress 1090) with a freshly cut Ag wire as the quasi-reference and a Pt wire as the counter electrode in an Ar environment. The Ag and Pt electrodes were sonicated in acetone, ethanol, and pure water (resistivity: 18 MΩ·cm) sequentially for 10 min in each step and then dried with N_2 gas. The Pt wire was further annealed with a hydrogen flame. The electrolyte (0.1 M $NaClO_4$) was degassed with Ar for 30 min before each measurement. The quasi-reference electrode was calibrated against a standard Ag/AgCl (in saturated KCl) reference electrode.

The electrochemical gate-controlled electron transport measurement was carried out using working, reference, and counter electrodes prepared in the same way as above. The two working electrodes, the substrate and tip, play the roles of source and drain electrodes, and the reference electrode resembles the role of gate electrode in field effect transistors (FET). The gate voltages in this article are quoted as the potential of the substrate with respect to the reference electrode, and thus they are opposite to the sign convention in the solid-state FETs. We note that despite the similarities between the electrochemical gating setup and conventional FETs, the operation mechanisms are different, as we will discuss later. To independently control the gate and source−drain bias voltages, a bipotentiostat was used. The electrochemical cell was made of Teflon, which was soaked in Piranha and then boiled in 18 MΩ·cm water three times to clean it. (Caution: Piranha solution reacts violently with most organic materials and must be handled with extreme care.) To minimize possible oxygen effects, the electron transport measurements were also performed in a glass chamber purged with Ar gas. A Peltier heating/cooling stage (Molecular Imaging Corp.) with a Lakeshore temperature controller was used to control the temperature of the sample cell. The controllable temperature range was between 5 and 35 °C. At each temperature, we waited for at least 30 min before starting transport measurements to allow the entire sample stage to reach thermal equilibrium.

The details of the STM break junction method were described elsewhere.[23] Briefly, it started with the normal STM imaging mode to survey the cleanness and flatness of the substrate, the sharpness of the tip, and the mechanical stability of the entire setup. Once a clean, sharp, and stable STM image was obtained, the normal STM feedback was switched off and a separate computer was turned on to control the tip movement. The tip was first pushed toward the substrate at a rate of 20−40 nm/s until the current between the tip and the substrate reached a preset value. It was then pulled away from the substrate until the current dropped to zero. The processes were repeated to generate a large number of transient conductance curves for statistical analysis.

We observed three types of transient curves (Figure 1). The first type was a smooth exponential decay due to electron tunneling between the tip and the substrate. The percentage of these decay curves was 70%, much higher than that observed for alkanedithiols in toluene,[23] indicating a lower probability of forming molecular junctions with the PTCDI molecules. The difference may be understood by the following consideration. The PTCDI molecules in the present work were preassembled on Au substrate from DMSO, and the PTCDI-coated substrate was then exposed to the solvent containing no PTCDI molecules for conductance measurements. In contrast, the previous

(18) Cui, X. D.; Primak, A.; Zarate, X.; Tomfohr, J.; Sankey, O. F.; Moore, A. L.; Moore, T. A.; Gust, D.; Harris, G.; Lindsay, S. M. *Science* **2001**, *294*, 571−574.
(19) Magoga, M.; Joachim, C. *Phys. Rev. B* **1997**, *56*, 4722−4729.
(20) Yaliraki, S. N.; Kemp, M.; Ratner, M. A. *J. Am. Chem. Soc.* **1999**, *121*, 3428−3434.
(21) Moresco, F.; Gross, L.; Alemani, M.; Rieder, K. H.; Tang, H.; Gourdon, A.; Joachim, C. *Phys. Rev. Lett.* **2003**, *91*, 036601/1−036601/4.
(22) Xu, B. Q.; Tao, N. J. *Science* **2003**, *301*, 1221−1223.
(23) Li, X. L.; He, J.; Hihath, J.; Xu, B. Q.; Lindsay, S. M.; Tao, N. J. *J. Am. Chem. Soc.* **2006**, *128*, 2135−2141.

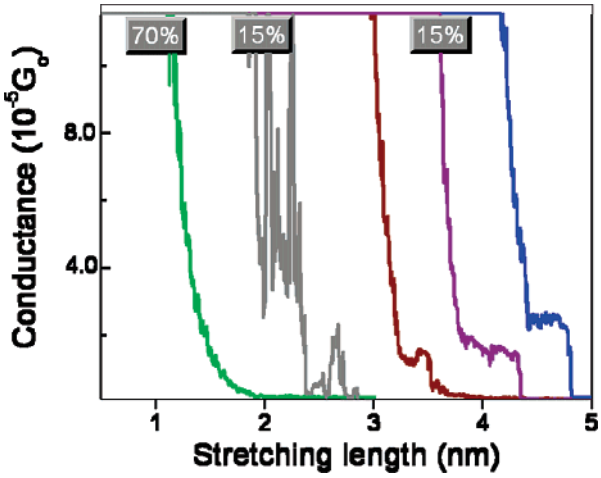

Figure 1. Typical transient current traces of T-PTCDI in 0.1 M $NaClO_4$ aqueous solution. The gate and source−drain bias voltages were held at 0.2 and 0.1 V, respectively.

studies were carried out in a solution containing 1 mM alkanedithiols, so that the molecules dissolved in the solvent could constantly diffuse to and adsorb onto the tip and substrate electrodes. The second type of transient curve was noisy and rapidly varying, probably because of mechanical vibrations of the setup, residual impurities in the sample cell, or unstable molecular junctions. The percentage of the noisy curves was around 15%. The exponential decay and noisy curves were either not recorded or removed after recording in the construction of the conductance histograms. The remaining 15% were curves with clear steps, which were used to construct conductance histograms.

To study the source−drain current (I_{sd}) vs electrochemical gate voltage (V_g) of individual molecular junctions, we also used a pull−hold method.[23,24] In this method, we manually drove the STM tip toward the substrate by controlling the piezoelectric transducer (PZT) with a precision variable voltage source and then pulled the tip away from the substrate. Once the lowest conductance plateau was reached, corresponding to the formation of a single molecular junction, we then fixed the tip position and recorded the current (I_{sd}) while sweeping the electrochemical gate voltage (V_g) with a fixed source−drain bias. This measurement required a mechanically stable system that frequently took several hours to reach. Since the gate can change the conductance of PTCDI by several orders of magnitude, we used a logarithmic current preamplifier to measure the individual $I_{sd}-V_g$ curves. The amplifier feedback used eight diodes (four for each direction of current) across a 1 GΩ resistor, giving rise to a linear response below 1 nA and a logarithmic response above 2 nA.[25] The current to voltage conversion was calibrated with a series of resistors (15 kΩ, 1 MΩ, 10 MΩ, 100 MΩ, and 1 GΩ) to yield a point by point calibration.

Results and Discussion

Cyclic Voltammograms. Figure 2 shows the cyclic voltammograms of phenylthiol-terminated PTCDI (T-PTCDI) and ethylthiol-terminated PTCDI (C-PTCDI) adsorbed on Au electrodes in 0.1 M $NaClO_4$. Both molecules show a pair of peaks near −0.6 V, corresponding to a reversible redox reaction. The pyridine-terminated PTCDI (P-PTCDI) desorbs from Au electrode at potentials more positive than the redox potentials, which prevented us from observing the redox peaks. One unique property of PTCDI molecules is that the two nitrogen positions are nodes in the π-orbital wavefunction,[26] providing enormous

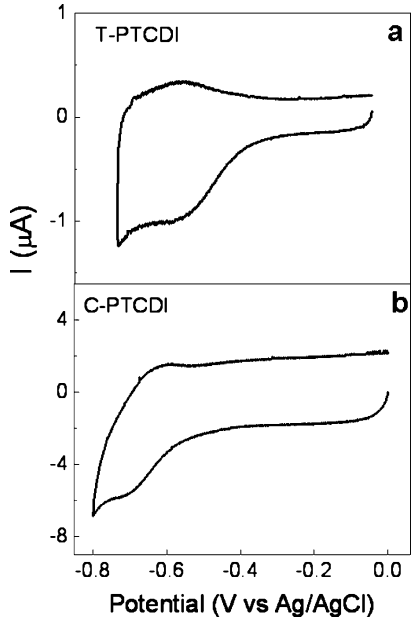

Figure 2. Cyclic voltammograms of T-PTCDI (a) and C-PTCDI (b) adsorbed on a Au electrode in 0.1 M $NaClO_4$ electrolyte in an Ar chamber. The potential scan rate was 0.2 V/s.

options for modifying the structures of the two side chains (but without significant alteration of the electronic structure of PTCDI). Such a side chain insensitive electronic property is consistent with the cyclic voltammetry measurement shown in Figure 2, where similar redox potentials are observed for two different PTCDI molecules. As calculated by density functional theory (B3LYP/6-31g*) using the Gaussian 03 package, the LUMO and HOMO of PTCDI molecules are located at −3.8 and −6.3 V vs vacuum energy level, respectively. The cyclic voltammetry also indicates that despite the different anchoring groups all three PTCDI molecules should possess the same alignment of the LUMO and HOMO levels relative to the Fermi level of the gold electrodes.

Conductance of PTCDI Derivatives Terminated with Different Anchoring Groups. We determined the conductance of the molecules by performing statistical analysis of the steps in the current transient curves (Figure 1). The conductance histograms revealed peaks that were used to determine the average conductance of a single molecule bound to two Au electrodes. Figure 3a compares the conductance histograms of C-PTCDI and T-PTCDI at zero gate voltage. The peak positions correspond to the most probable conductance values of the molecules, and the broad widths of the peaks are due to large variations in the microscopic details of the molecule−electrode contacts.[27] The conductance values of C-PTCDI, T-PTCDI, and P-PTCDI determined from the histograms are $0.78 \times 10^{-5}G_0$, $1.75 \times 10^{-5}G_0$, and $5.6 \times 10^{-5}G_0$, respectively, where $G_0 = 2e^2/h \approx 77.4\ \mu S$, with e as the electron charge and h as the Planck constant. The three PTCDI derivatives have similar electronic states as shown by the cyclic voltammograms and the theoretical calculation, but P-PTCDI is ∼7 times more conductive than C-PTCDI. The large conductance difference can be attributed to different electronic couplings between the molecules and the electrodes, mainly caused by the different anchoring groups.[28] P-PTCDI has the largest conductance, which

(24) Xu, B. Q.; Zhang, P. M.; Li, X. L.; Tao, N. J. *Nano Lett.* **2004**, *4*, 1105−1108.
(25) He, J.; Sankey, O.; Lee, M.; Tao, N. J.; Li, X. L.; Lindsay, S. *Faraday Discuss.* **2006**, *131*, 145−154.
(26) Kazmaier, P. M.; Hoffmann, R. *J. Am. Chem. Soc.* **1994**, *116*, 9684−9691.
(27) Xiao, X. Y.; Xu, B. Q.; Tao, N. J. *Nano Lett.* **2004**, *4*, 267−271.

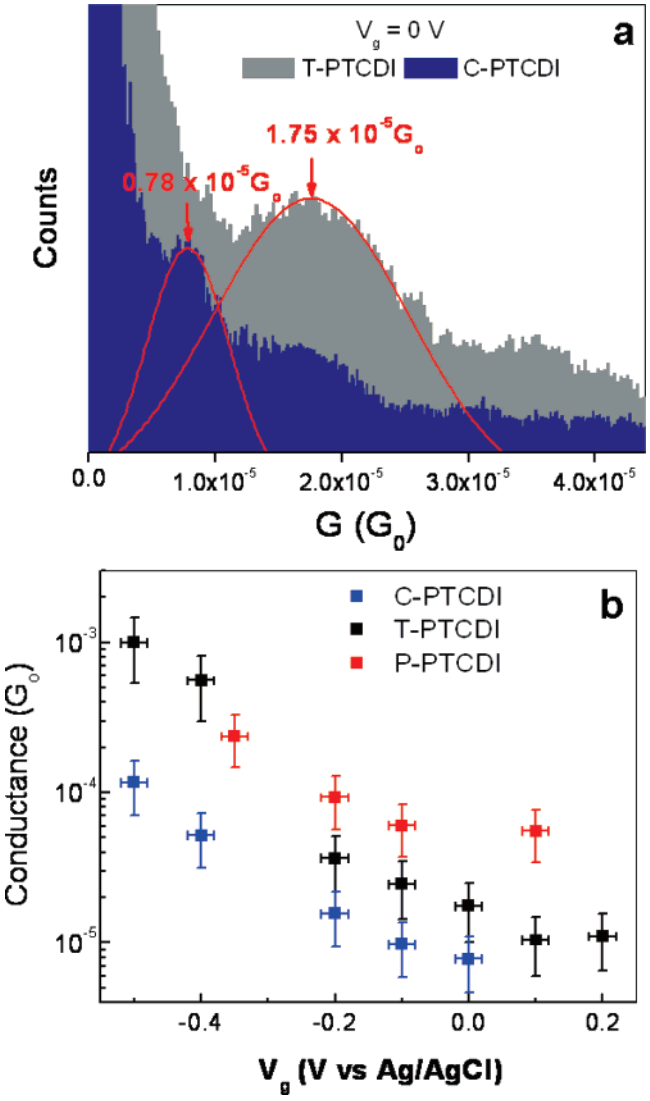

Figure 3. (a) Conductance histograms of C-PTCDI and T-PTCDI measured in 0.1 M $NaClO_4$ at 0.1 V bias and 0 V gate voltage. The solid lines are Gaussian fits. (b) Average conductance values vs gate voltage for C-PTCDI, T-PTCDI, and P-PTCDI. The conductance error bars are the widths of first conductance peaks in the histograms. The gate voltage error bars are the maximum drift in the potential of the Ag quasi-reference electrode.

may be partially due to the shortest coupling distance provided by the pyridine group. However, distance is not the only parameter that determines the coupling efficiency. For example, phenylthiol is longer than ethylthiol, but T-PTCDI is more conductive than C-PTCDI. The larger conductance of T-PTCDI can be attributed to the π-conjugated structure of the phenylthiol anchoring group, which provides more efficient coupling than the two saturated carbon bonds in the ethylthiol group.[29] Note that, although the phenylthiol and pyridine are conjugated within themselves, they are not conjugated with the PTCDI backbone because of the node at the nitrogen position.

Electrochemical Gate Effect. Figure 3b shows semilogarithmic plots of conductance vs gate voltage for the three PTCDI derivatives, and the figure shows a rapid increase in the conductance when decreasing the gate voltage below −0.1 V. The error bars for the conductance in Figure 3b are the full widths at half-maximum (fwhm) values of the first conductance peaks in the histograms, which reflect the distribution of different contact geometries. The gate voltage error bars are mainly caused by the drift of the Ag quasi-reference electrode. The lowest gate voltages studied for T- and C-PTCDI were about −0.5 V, below which the percentage of curves showing steps dropped sharply. This is likely due to the weakening of the S−Au bond as the voltage decreases to the regime of reductive desorption of the S−Au bond.[30] For P-PTCDI, the lower limit for gate voltage was ∼−0.4 V because of the potential-induced desorption of pyridine from Au electrodes.[31−33]

An important parameter that describes the effectiveness of gate control for a field effect transistor is subthreshold slope. For an ideal ballistic MOSFET, the subthreshold slope is 60 mV/decade, or 10-fold change in the source−drain current for a gate voltage change of 60 mV. For molecular FETs, Damle et al.[34] have predicted a slope of 300 mV/decade. The three PTCDI derivatives all show a large gate effect, but their subthreshold slopes are different. From the semilogarithmic plots of I_{sd} vs V_g shown in Figure 3b, we determined the subthreshold slopes of the three molecules. T-PTCDI has the smallest slope, ∼180 mV/decade, whereas P-PTCDI and C-PTCDI have slopes around 400 mV/decade at room temperature. We note that the transport and electrochemical gating mechanisms in redox molecules are different from those in conventional MOSFETs, and the 60 mV lower limit in the subthreshold slope in a MOSFET may not apply to the molecular system.

The above statistical analysis provides an average picture of many molecular junctions with different contact configurations. The pull−hold method reveals more details associated with each of the individual molecular junctions (Figure 4). For example, there is a large run-to-run variation in the individual $I_{sd}-V_g$ curves, which can be attributed to the variation in the contact geometry. We observed also a small but finite hysteresis in $I_{sd}-V_g$ curves. Hysteresis has been found in the $I-V$ curves of bipyridyl-dinitro oligophenylene-ethynylene dithiol in vacuum using a break junction method.[35] We believe that the hysteresis in the present system is due to redox-induced changes in the molecule and local environment, such as counterion redistribution. In fact, much larger hysteresis effects have been observed in other redox molecules, such as oligoaniline,[14] oligothiophene,[36] and ferrocene.[37] The smaller hysteresis in PTCDI may be understood based on the following considerations. First, PTCDI is structurally rigid so that structural relaxation associated with the redox reaction is small. Second, an electron added to PTCDI is delocalized over the extended perylene rings, which induces a smaller amount of polarization of the surrounding solvent molecules than the cases where the electron is localized.

(28) Chen, F.; Li, X. L.; Hihath, J.; Huang, Z. F.; Tao, N. J. *J. Am. Chem. Soc.* **2006**, *128*, 15874−15881.
(29) Datta, S.; Tian, W. D.; Hong, S. H.; Reifenberger, R.; Henderson, J. I.; Kubiak, C. P. *Phys. Rev. Lett.* **1997**, *79*, 2530−2533.
(30) Sumi, T.; Uosaki, K. *J. Phys. Chem. B* **2004**, *108*, 6422−6428.
(31) Cunha, F.; Tao, N. J.; Wang, X. W.; Jin, Q.; Duong, B.; D'Agnese, J. *Langmuir* **1996**, *12*, 6410−6418.
(32) Mayer, D.; Dretschkow, T.; Ataka, K.; Wandlowski, T. *J. Electroanal. Chem.* **2002**, *524−525*, 20−35.
(33) Wandlowski, T.; Ataka, K.; Mayer, D. *Langmuir* **2002**, *18*, 4331−4341.
(34) Damle, P.; Rakshit, T.; Paulsson, M.; Datta, S. *IEEE Trans. Nanotechnol.* **2002**, *1*, 145−153.
(35) Lortscher, E.; Ciszek, J. W.; Tour, J.; Riel, H. *Small* **2006**, *2*, 973−977.
(36) Xu, B. Q.; Li, X. L.; Xiao, X. Y.; Sakaguchi, H.; Tao, N. J. *Nano Lett.* **2005**, *5*, 1491−495.
(37) Xiao, X. Y.; Brune, D.; He, J.; Lindsay, S.; Gorman, C. B.; Tao, N. J. *Chem. Phys.* **2006**, *326*, 138−143.

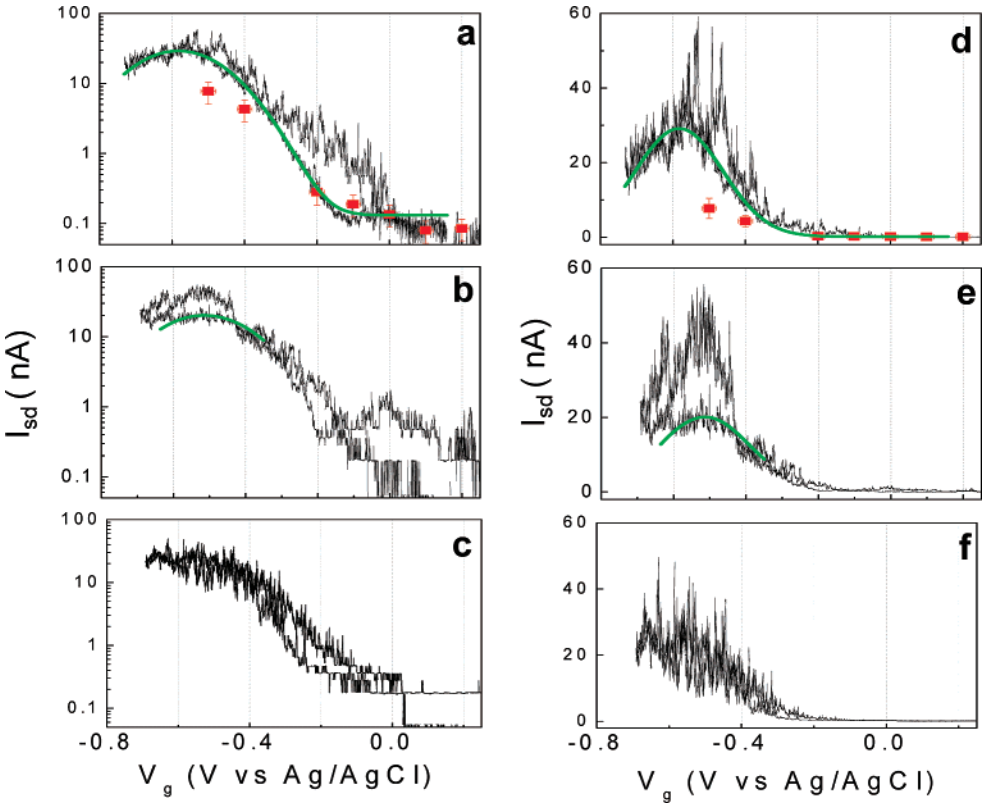

Figure 4. Source−drain current (I_{sd}) vs gate voltage (V_g) of three independently formed T-PTCDI junctions in logarithmic (a−c) and linear (d−f) scales. For a given molecular junction, repeated gate voltage cycles show similar $I_{sd}-V_g$ curves, and thus only one cycle is shown here for clarity. Data obtained from the peak positions of the conductance histograms are also plotted as filled squares in a and d for comparison. Source−drain bias was fixed at 0.1 V, and the gate sweeping rate was 0.1 Hz in the measurements.

Similar to the case of the statistical method, the lowest gate voltage in the pull−hold method was also limited by the reductive desorption of the S−Au bond. However, since the pull−hold method requires only a few seconds, we were frequently able to push the limit to −0.7 V. The expanded gate voltage window covers the redox potential of the molecules and allowed us to observe a peak in the $I_{sd}-V_g$ near the redox potential. Despite run-to-run variations, 65% (73 out of 112) of individual $I_{sd}-V_g$ curves show a pronounced peak (Figure 4a,b), and the remaining 35% of the curves are either noisy or show less pronounced peak feature (Figure 4c). The peak current fluctuates considerably, far greater than the noise level of the current amplifier, which may be associated with the fluctuation in the local distribution of the ions. The average peak current is ~500 times greater than that at 0.2 V gate voltage. Since the peak position fluctuates from run to run, a histogram of the peak positions was constructed (Figure 5), showing that the most probable peak position is around −0.55 V, which is close to the redox potential of the molecules (Figure 2a).

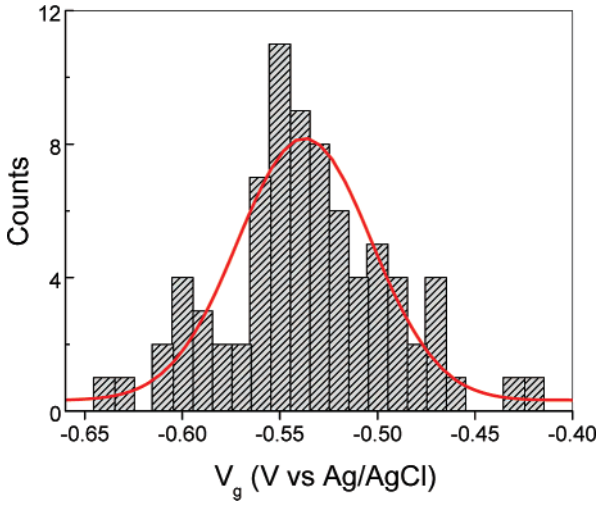

Figure 5. Distribution of the peak positions in the individual $I_{sd}-V_g$ curves. Solid red line is a Gaussian fit.

We carried out the same measurements on C-PTCDI and observed a similar large gate effect (Figure 6). For P-PTCDI, it remained difficult to lower the gate voltage below the redox potential because of the potential-induced desorption of the pyridine groups on Au electrodes.

Control Experiments. We carried out control experiments to further confirm that the observed large gate effect is indeed due to the redox activity of the PTCDI molecules. The first control experiment was to measure tunneling current between the tip and substrate in the absence of molecules as a function of gate voltage. We performed STM break junction measurement in 0.1 M $NaClO_4$ and found that more than 96% of individual curves are smooth exponential decays (Figure 1). The remaining 4% show kinks or steplike features, which are random, and the corresponding histogram does not exhibit obvious peaks. We attributed these features to impurities and mechanical vibrations in the system. Similar to the pull−hold method, we recorded the tunneling current flowing between the tip and substrate as a function of electrochemical gate voltage, and we did not observe gate voltage dependent tunneling current, which is in sharp contrast to the large gate effect found in the PTCDI derivatives.

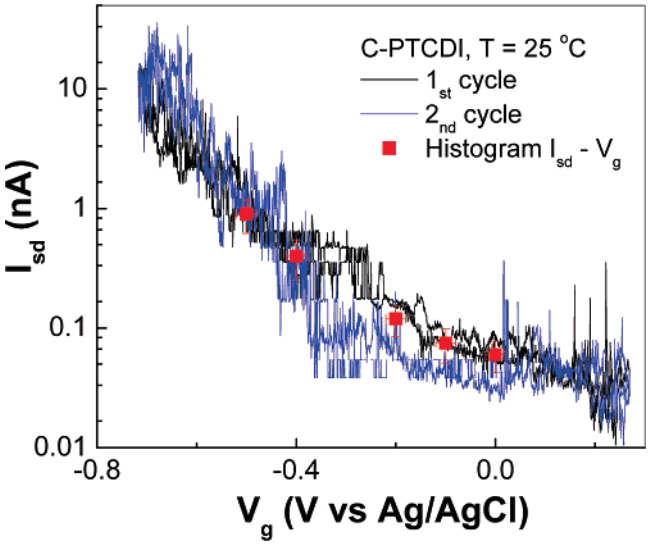

Figure 6. Source−drain current (I_{sd}) vs gate voltage (V_g) for a C-PTCDI junction. Repeatable cycles of the gate voltage between −0.7 and 0.2 V show variations in the current but similar gate dependence (black and blue lines). Source−drain bias was fixed at 0.1 V in the measurements.

The second control experiment was to perform the measurement on octanedithiol under the same conditions. We first checked the cyclic voltammogram of octanedithiol adsorbed on Au electrodes and found no electrochemical reactions within the studied potential window. We then carried out the conductance measurement using the statistical method at various gate voltages. Figure 7 shows the conductance histograms obtained by holding the gate voltages at −0.6 V and +0.5 V, respectively. The peaks marked by "HC" and "LC" are attributed to different contact geometries.[23] Within this large window of gate voltage, no obvious shift was observed in the conductance of octanedithiol. We also measured the gate effect of individual octanedithiol junctions and found little change in the current over the entire gate voltage window. The lack of gate effect in octanedithiol is mainly because (1) the HOMO−LUMO gap of the molecule is large and the Fermi levels of the electrodes are far away from the HOMO and LUMO and (2) octanedithiol is short, which causes substantial screening of gate field.[38]

Temperature Effect. Since P-PTCDI is stable on Au electrodes within a small gate voltage window, we focused the temperature dependence measurement on T-PTCDI and C-PTCDI. For both T-PTCDI and C-PTCDI, the conductance increases with temperature and the amount of increase depends on gate voltage (Figure 8). At positive gate voltages, the conductance increases with temperature. Decreasing the gate voltage to the redox potential diminishes the temperature effect. For example, at $V_g = 0.2$ V the conductance of T-PTCDI at 5 °C is $\sim 0.6 \times 10^{-5} G_0$, but it increases to $\sim 2.6 \times 10^{-5} G_0$ when increasing temperature to 35 °C. In contrast, the conductance changes little with temperature when holding the gate voltage near −0.5 V (Supporting Information, S1 and S2).

To rule out the possibility that the observed temperature effect originates from possible thermal drift in the potential of the reference electrode and/or temperature dependence of the molecule−electrode coupling strengths, we measured the cyclic voltammograms of T-PTCDI and C-PTCDI adsorbed on Au electrodes at different temperatures. We found that the redox peaks (positions and areas) were insensitive to temperature (Supporting Information, S3). These observations show that the reference electrode is stable within the temperature range and no measurable desorption takes place as a result of changing temperature.

The observation of temperature dependence of the PTCDI conductance indicates that electron transport in PTCDI molecules involves thermal activation. By fitting $\ln(G)$ vs $1/T$ with a linear function, we extracted thermal activation energy at different gate voltages (Figure 9a). Similar to the previous section, the error bars are determined from fwhm of the Gaussian fits for the first peak in the conductance histogram, reflecting the distribution of different contact geometries. Figure 9b plots the activation energy E_a as a function of gate voltage for T-PTCDI and C-PTCDI.

To determine the solvent effect, we performed the conductance measurement as a function of temperature in toluene.[14] Figure 10 is the conductance of T-PTCDI vs $1/T$. Within the temperature window available in our current experimental setup, the conductance value is independent of temperature. The error bars in the figure were determined by fwhm of the first conductance peak fitted with a Gaussian function.

The lack of temperature effect of the redox molecules in nonpolar solvents suggests the importance of the surrounding water molecules in the electron transport of redox molecules in aqueous electrolytes. The coupling of redox states to the polarization of solvent molecules plays a critical role in the electron-transfer phenomena as described by Marcus theory.[39] The gate dependence of the activation energies for both T-PTCDI and C-PTCDI can be fit by

$$E_a \propto \frac{(V_g - V_0)^2}{4\lambda} \qquad (1)$$

where V_0 is the redox potential and λ is the only fitting parameter (Figure 9c). This expression resembles the activation energy predicted by Marcus theory, in which λ is reorganization energy due to the polarization of the surrounding polar solvent molecules and the structural relaxation of the molecule.[39] For the PTCDI derivatives studied here, the LUMO is delocalized and the structure is rigid, and therefore the solvent polarization is expected to be the dominant contribution to the reorganization energy. By linear fitting E_a vs $(V_g - V_0)^2\lambda$, was found to be ~0.4 and ~0.6 eV for T-PTCDI and C-PTCDI, respectively, which are reasonable values for the outer shell (solvent polarization) component of the reorganization energy found in electron-transfer phenomena.

Schmickler et al.[8,40] considered a redox molecule adsorbed on a metal substrate underneath an STM tip. They predicted a resonant tunneling when the LUMO (oxidized states) of the molecule is brought to the Fermi levels of the substrate and tip. Because of resonant tunneling, the current gives rise to a peak in the current vs gate voltage plot, which appears to agree with our observation. However, the resonant tunneling theory predicts that the peak occurs at $V_g = V_0 - \lambda/e$, well below the redox potential. In contrast, the maximum current observed in

(38) Li, X. L.; Xu, B. Q.; Xiao, X. Y.; Yang, X. M.; Zang, L.; Tao, N. J. *Faraday Discuss.* **2006**, *131*, 111−120.
(39) Kuznetsov, A. M.; Ulstrup, J. *Electron Transfer in Chemistry and Biology: An Introduction to the Theory;* Wiley: Chichester, 1999.
(40) Schmickler, W. *Surf. Sci.* **1995**, *335*, 416−421.

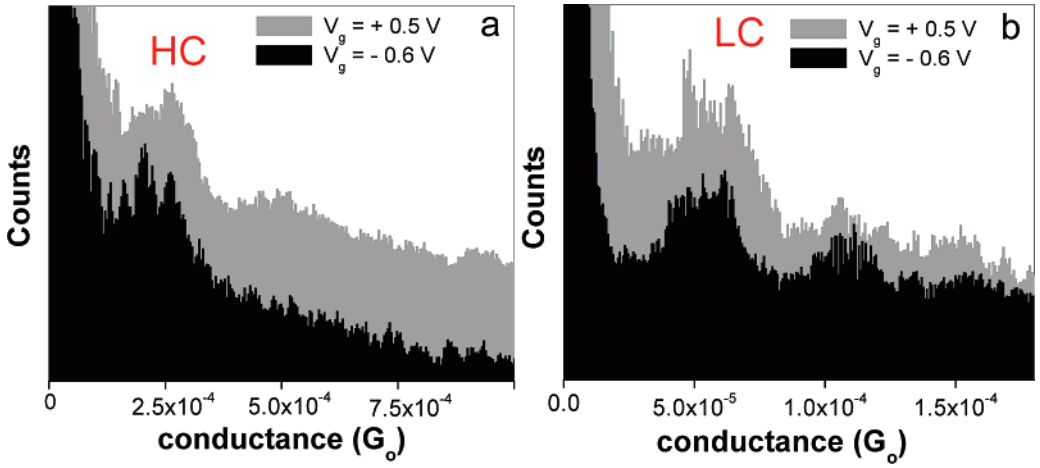

Figure 7. Conductance histograms of octanedithiol obtained in 0.1 M $NaClO_4$ at a gate voltage of −0.6 V and +0.5 V. Both H (a) and L (b) conductance values are independent of the gate voltage. Bias was fixed at 0.1 V in these measurements.

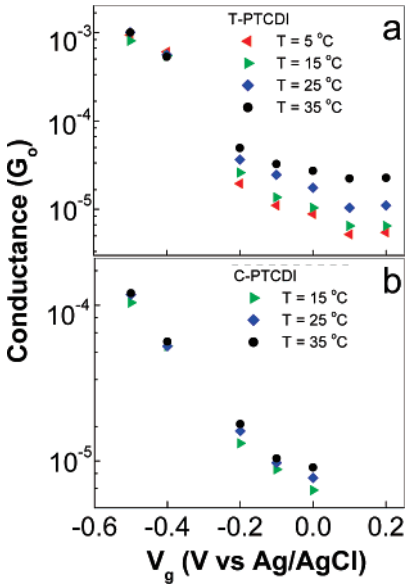

Figure 8. Conductance of T-PTCDI (a) and C-PTCDI (b) vs gate voltage at different temperatures. Temperature dependence is distinct at more positive gate voltages and vanishes when the gate voltage is decreased to the redox potential.

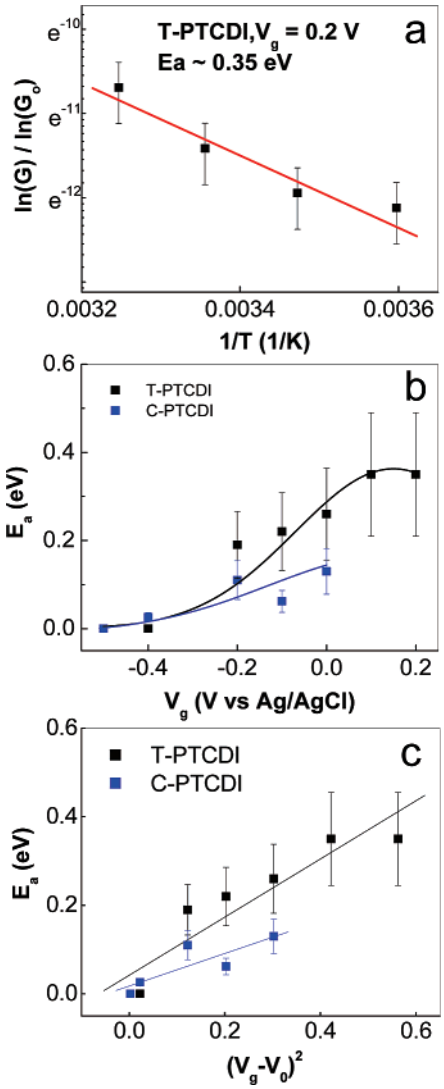

Figure 9. (a) Conductance G vs temperature $1/T$ for T-PTCDI at $V_g = 0.2$ V. (b) Activation energy vs gate voltage for T-PTCDI (black) and C-PTCDI (blue). (c) Dependence of activation energy on gate voltage.

our experiments occurs near the redox potential. An alternative model by Kuznetsov and Ulstrup[10] is a thermally activated two-step sequential process in which an electron transfers from one electrode into the molecule to reduce the molecule and then transfers out to the second electrode to reoxidize the molecule. This theory is supported by recent STM measurements.[41] Its prediction that a maximum transport current occurs near the redox potential is in agreement with our data. The two-step model further predicts an increase in the conductance with temperature,[10,42] which also explains our data. However, the observed gate effect and temperature dependence cannot satisfactorily fit with the equations developed from the two-step model. One possible reason is that many details in the molecular junctions are not explicitly included in the two-step model. Examples include ionic screening because of the proximity of the source and drain electrodes, position of the redox center, and the coupling between the redox center and the electrodes, which could affect the $I_{sd}-V_g$ curves and the detailed temperature dependence.

(41) Chi, Q. J.; Farver, O.; Ulstrup, J. *Proc. Natl. Acad. Sci. U.S.A.* **2005**, *102*, 16203−16208.
(42) Kuznetsov, A. M.; Ulstrup, J. *J. Electroanal. Chem.* **2004**, *564*, 209−222.

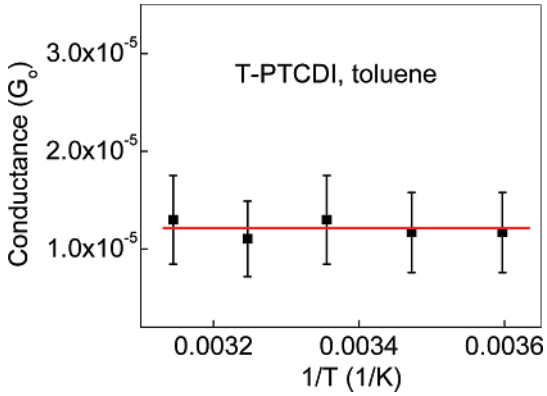

Figure 10. Conductance of T-PTCDI measured in toluene vs temperature. Within the available temperature window, the conductance of T-PTCDI obtained in toluene is independent of temperature. The bias was 0.1 V in the measurements.

Conclusions

In summary, we have studied electron transport in single redox molecules, PTCDI derivatives terminated with different anchoring groups, as a function of electrochemical gate voltage and temperature in polar and nonpolar solvents. Two methods have been used: one is based on analyzing a large number of molecular junctions statistically, and the other one is to directly measure the current through each of the individual molecular junctions. The current through each PTCDI derivative increases quickly with decreasing gate voltage and reaches a peak near the redox potential. There is a small hysteresis between forward and reverse sweeping of the gate voltage, which is attributed to the structural reorganization of the redox molecules. Despite the similarities in the gate dependence for the three PTCDI derivatives, their subthreshold slopes are different. In addition, the conductance is sensitive to the anchoring groups of the PTCDI derivatives.

Electron transport in these molecules depends on the temperature in the aqueous electrolyte but is independent of temperature in a nonpolar solvent, suggesting a strong coupling of the redox states to the polarized water molecules. We have obtained thermal activation energy of the electron transport as a function of gate voltage, from which the reorganization energy associated with the polarization of water molecules was extracted. Our results suggest that the electron transport in these redox molecules is a thermally activated two-step sequential process, in which electrons, assisted by thermal fluctuations, tunnel into the molecule from one electrode and out of the molecule to the second electrode.

Acknowledgment. We thank Mark Ratner for helpful discussions, and NSF (CHM-0554786) (X.L.), DARPA via AFOSR (#AF8650-06-C-7623) (J.H. and T.M.), and DOE (DE-FG02-01ER45943) (F.C.) for financial support.

Supporting Information Available: Conductance histograms and transient conductance traces at different temperatures and gate voltages, cyclic voltammograms at different temperatures. This material is available free of charge via the Internet at http://pubs.acs.org.

JA072990V